Localized damage detection in a large-scale moment connection using a strain gauge sensor network

E. Labuz[a], S. Pakzad[a], D. Wurst[b]
[a]Dept. of Civil and Environmental Engineering, Lehigh University, Bethlehem, PA USA
[b]Dept. of Civil and Environmental Engineering, Rowan University, Glassboro, NJ USA

ABSTRACT

In order to maintain healthy structures, it is important to find means of Structural Health Monitoring (SHM) that are effective, economical, and easy to implement. A localized damage detection algorithm based on measured data from a densely clustered sensor network has been previously presented. This method has been validated using both wired and wireless accelerometers applied to a small-scale idealized beam-column connection. However, to progress towards real-world implementation, there is a need to verify that this algorithm is effective and applicable for full-scale structures with unknown progressive damage. Moreover, it is important to verify the use of other commonly used sensor types, in this case strain gauges, which represent different response parameters. In this paper, the performance of the damage detection algorithm is evaluated for a large-scale steel moment connection constructed at the ATLSS Center at Lehigh University, which was being tested for use in an earthquake-prone structure. This test specimen was instrumented with a network of strain gauges and cyclically loaded to failure. The strain responses from the test are analyzed using the local damage detection algorithm. The resulting changes in the damage indicating parameters compared to the damage observations to both determine the point of earliest detection and to verify the locations of the damage. By successfully implementing this local damage detection algorithm using strain gauges instrumented on a large-scale structure, the versatility of this method is demonstrated.

Keywords: Structural Health Monitoring, localized damage detection, sensor network, strain gauge

1. INTRODUCTION

Building codes and design methodologies have been created to ensure the design of structures that are safe for public use. However, structures are susceptible to deterioration over time or unexpected damage in extreme loading cases. Structural Health Monitoring (SHM) methods attempt to detect and locate structural damage in order to prevent structural failures. The ability to localize damage at early stages will also result in the benefit of more economical repairs.

While traditional Nondestructive Evaluation (NDE) methods [1] provide effective means of damage identification, these methods require *a priori* knowledge of damage existence and location. Furthermore, NDE techniques are subject to the trained eye of the inspector, sometimes require the use of costly, complex equipment, and provide only a temporary means of SHM. Technological advancements in wireless sensors have allowed for the development of new SHM methods that can be applied on a temporary or semi-permanent basis [2, 3, 4, 5, 6]. These sensor networks are especially applicable for the implementation of vibration based SHM methods, which rely on changes in modal properties to reveal changes in the physical properties of the structure, i.e. structural damage [7, 8]. However, modal properties only reflect global damage, requiring a greater amount of damage before detection is feasible. Additionally, these global-based damage detection methods require knowledge of specific structural properties, including mass, stiffness, or damping ratio, for which it is often difficult to determine correct values [9, 10, 11, 12]. Moreover, environmental influences may cause larger changes to the vibration properties of the structure than the onset of damage, making modal properties unreliable damage parameters [2].

Some SHM methods focus on local damage detection. However, these methods, for example the damage locating vector (DLV) method [13], also require the knowledge of structural properties or require homogeneity of the structural properties as in the two-dimensional gapped smoothing method [14].

Sensors and Smart Structures Technologies for Civil, Mechanical, and Aerospace Systems 2011, edited by Masayoshi Tomizuka, Chung-Bang Yun, Victor Giurgiutiu, Jerome P. Lynch, Proc. of SPIE Vol. 7981, 79813Q
 · doi: 10.1117/12.880752

A new localized damage detection method has been proposed that requires neither known properties of the structure, nor homogeneity of these properties [15]. The method operates on the principle that a structure exhibits linear-elastic behavior. The structural response at any one point on the structure can then be related to the response at other locations on the structure using regression analysis. Once damage has occurred this relationship will be altered for certain locations on the structure depending on the location of damage. By comparing the relationships from the damaged state to that of the baseline healthy state, a pattern of changes can be identified that will determine the location of the damage. This method has been validated using a simulated and experimental small-scale beam-column connection [15]. The algorithm has also been used to compare the performance of a wireless accelerometer sensor network to that of wired accelerometers, resulting in effective damage detection in both networks [16].

The model analyzed in these previous applications has idealized the damage; the beam is replaced with a member of known characteristics to simulate damage. Also, the entire beam section, designed to mimic the portion of the beam closest to the connection, has uniform damage, which is unlikely to occur in a real structure. Therefore, there is a need to verify this method for full-scale structures exhibiting more realistic damage scenarios. Moreover, it is important to verify the use of other commonly used and affordable sensor types, in this case strain gauges, which represent different response parameters. In this paper, the performance of the damage detection algorithm is evaluated for a large-scale steel moment connection constructed at the Advanced Technology for Large Structural Systems (ATLSS) Center at Lehigh University, which was being tested for use in an earthquake-prone structure. This test specimen was instrumented with strain gauges and cyclically loaded to failure. The strain responses were analyzed using the local damage detection algorithm to identify the progression of damage.

2. LARGE-SCALE MOMENT CONNECTION TESTING

2.1. Experimental Test Set-Up

Lehigh University was commissioned to test a new beam-column connection design for performance evaluation. Because the design is to be implemented in a California hospital, it is subject to the seismic qualification requirements as set for by the Office of Statewide Planning and Development (OSHPD) [17]. According to these requirements, the specimen must sustain at least two full cycles of an inelastic drift angle of 0.03 radians and at least two full cycles of an interstory drift angle of 0.04 or more radians without failure [17]. The beam-column was attached to the strong wall and strong floor at the ATLSS Center at Lehigh University, with two hydraulic actuators placed at the end of the beam for loading, as seen in Figure 1. The loading was applied cyclically with increasing drift sequences as follows: first, a drift of 0.00375 rad. was used for six cycles, followed by six cycles of 0.005 rad. drift, six cycles of 0.0075 rad. drift, four cycles at 0.01 rad., two cycles at 0.015 rad., two cycles at 0.02 rad., two cycles at 0.03 rad., two cycles at 0.045 rad., and then two cycles at increments of 0.01 rad. until failure [17]. Notes were taken throughout testing indicating the subjective amount and location of the damage that occurred during each drift sequence.

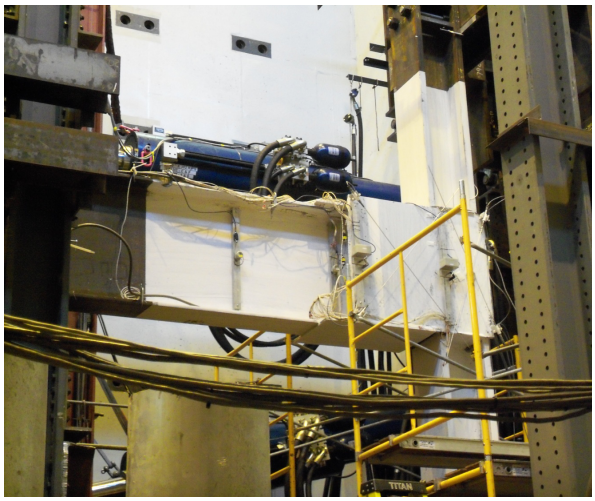

Figure 1. The beam-column test set-up utilizing the strong wall at the ATLSS Center

For the purpose of the research presented here, the test specimen was instrumented with a network of five[1] strain gauges as shown in Figure 2. For the location of the gauges in the beam, third points were taken from the side plate to the end of the beam to place gauges 32 and 33 on the top flange of the beam. Gauge 34 is located directly below gauge 32, on the bottom flange of the beam. The length of the column from the edge of the side pate to the strong wall connection was measured, and gauges 35 and 36 were placed on the outside flange at the top and bottom midpoints, respectively. The resulting strain responses were used to apply the proposed algorithm for indentifying the existence and location of damage in comparison to the observed damage notes.

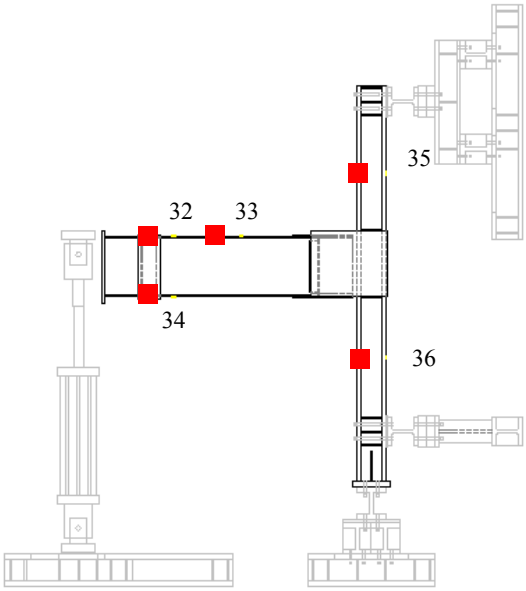

Figure 2. The beam-column test set-up and locations of five strain gauges

2.2. Observed Damage Results

The observed damage notes that were recorded during each drift sequence are presented in Table 1. Each drift sequence was assigned a damage class, with "Damage Class 1" corresponding to the first drift in which visible damage was observed. Figure 3 shows the progressive onset of structural damage due to increasing drift angles, starting with damage class 3 through failure.

[1] The number of gauges in the network was limited by the number of remaining channels in the data acquisition system beyond the sensors used for the primary purpose of the test.

Table 1. Damage classification based on the corresponding drift angles and damage description

Damage Class	Angle of Drift (radians)	Damage Observations
00	0.00375	None
0	0.005	None
1	0.0075	Onset of yielding under bottom of cover plate
2	0.01	Some slight yielding on the beam flange (extreme fiber) More yielding on the bottom cover plate
3	0.015	Yielding in the web about 1/5 of beam depth More yielding on the bottom cover plate Yielding in the through-thickness of beam flange Yielding in the top and bottom of beam flange
4	0.02	Web yielding of beam increased to 1/3 beam depth More yielding on the bottom cover plate More yielding on the beam flanges (top and bottom of both) Small crack (1/2in) in top cover plate to beam weld (bottom side) 2 small crack (1in) in top cover plate-to-beam weld No crack in base metal
5	0.03	Extremely yielding in the bottom cover plate Considerable yielding in beam bottom flange Web yielding more than 1/3 beam depth Top cover plate separated from beam Crack of top cover plate-to-beam weld (bottom side) opened up to 2in Cracks of top and bottom cover plate-to-beam weld (top side at cut-out) opened more than 2.5in
6	0.045	Web start to buckle Top flange start to buckle Bottom cover plate separated from the beam Plastic hinge completely formed Bottom cover plate-to-beam weld crack propagated Bottom flange started to buckle (at the end of cycle) Web buckled at lower depth of beam Small crack in side plate-to-column weld (left side)
7	0.05	Top flange buckling increased Web buckling increased Bottom flange buckling increased Bottom web buckling increased Crack in cover plate-to-beam weld stopped where the beam-to-side plate weld starts
8	0.06	Top cover plate-to-beam weld crack propagated to the base metal (beam flange) about 1/4in
9	0.07	Fracture from the bottom flange propagated into the web more than half the depth of beam

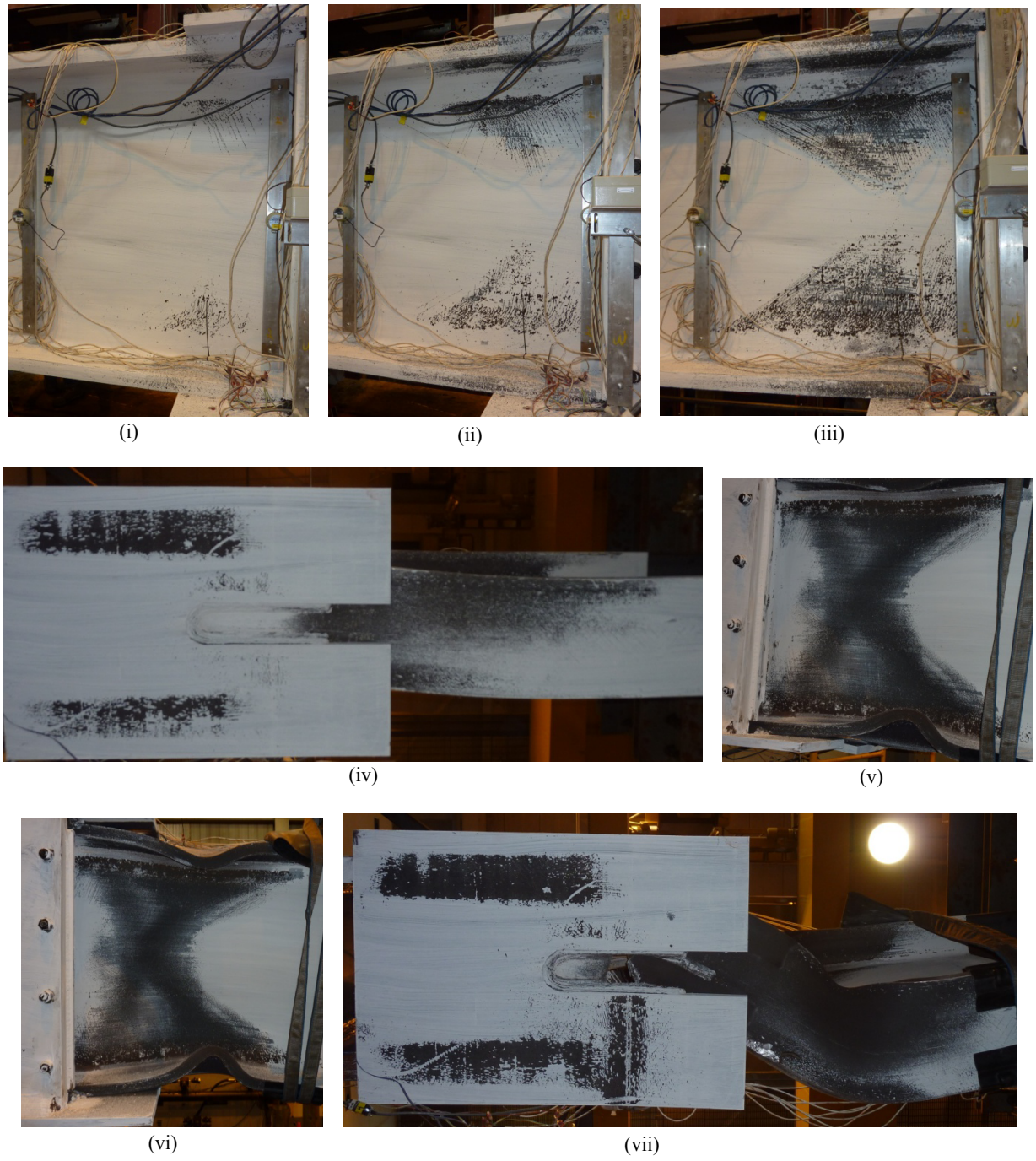

Figure 3. Damage severity at damage classes 3 (i), 4 (ii), 5 (iii), 6 (iv), 7 (v), 8 (vi), and 9 (vii)

3. IMPLEMENTATION OF THE LOCAL DAMAGE DETECTION ALGORITHM

3.1. Local Damage Detection Algorithm

The local damage detection algorithm implemented in this research utilizes linear regression analysis to quantify the linear relationship between strain responses at different points along the structure. The linear regression model is represented by Equation 1:

$$u_j(t_k) = \beta_{ij} + \alpha_{ij} \cdot u_i(t_k) + \varepsilon_{ij}(t_k) \quad (1)$$

where:

$u_i(t_k)$, $u_j(t_k)$ = structure's response at nodes i and j
β_{ij} = intercept value between nodes i and j
α_{ij} = influence coefficient between nodes i and j
ε_{ij} = error of the regression model

The influence coefficients from linear regression are the parameters used to determine the existence of damage. With the onset of damage, the physical characteristics of the structure begin to change, a change that is reflected in the influence coefficients. The pattern in which these changes occur reveals the location of the damage. The general approach for this method is outlined in Figure 4.

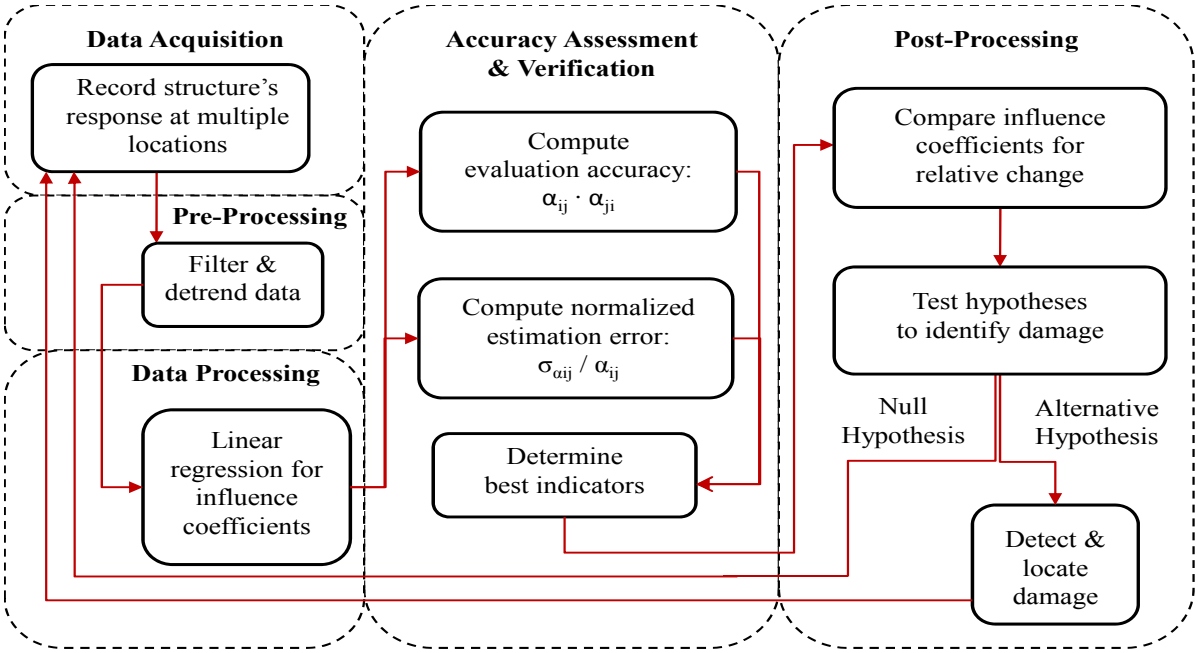

Figure 4. Methodology for the localized damage detection algorithm

The algorithm also employs different methods of checking the accuracy of the calculated α_{ij} values. This includes the estimation accuracy (EA) as well as the normalized estimation error (γ). These values indicate how accurate the linear relationships between sensor nodes are, and if their α_{ij} values are reliable when comparing coefficients. Theoretically, if the model had no error, corresponding coefficients, α_{ij} *and* α_{ji}, would be the reciprocal of one another. By multiplying the coefficients together, the EA can be determined. The closer to one this value is, the more accurate the α_{ij} values will be. The noise within the data used to calculate the coefficient is taken into consideration in γ. The closer to zero this value is, the less noise within a set of data, and the more accurate the coefficients are. These parameters are defined in Equations 2 and 3, respectively:

$$EA_{ij} = \alpha_{ij} \cdot \alpha_{ji} \quad (2)$$

$$\gamma_{ij} = \frac{\sigma_{\alpha_{ij}}}{\alpha_{ij}} \quad (3)$$

where:

EA_{ij} = influence coefficient between nodes i and j
γ_{ij} = normalized estimation error between nodes i and j
$\sigma_{\alpha_{ij}}$ = standard deviation of α_{ij}

3.2. Results of the Local Damage Detection Algorithm

Prior to processing the data through the algorithm, the strain responses were considered in comparison to one another as well as versus time. Figure 5 shows examples of strain versus strain plots for the two gauges on the column (i) and two of the gauges on the beam (ii). Figure 5(i) shows a case in which the relationship between the two responses remains mostly linear throughout all cycles with small changes in slope over time. Figure 5(ii), however, shows the result of excessive yielding, causing the gauges to reveal a nonlinear relationship in later cycles. Portions of the data which best mirrored a linear relationship were used in implementation of the algorithm in order to minimize the error term in the regression model, thus increasing the accuracy of the parameters.

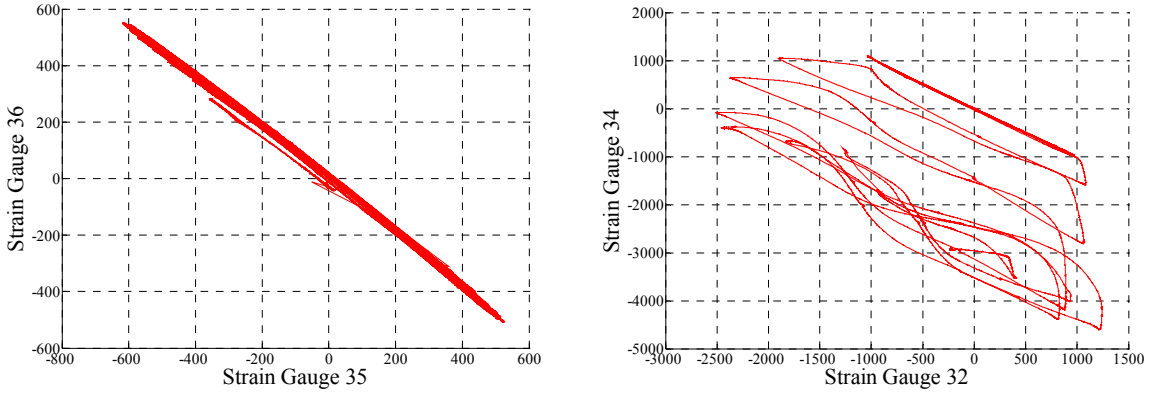

Figure 5. Strain gauges plotted against one another: (i) strain gauge 36 vs. strain gauge 35, (ii) strain gauge 34 vs. strain gauge 32

Figure 6 shows a plot of one of the strain responses (node 32) versus time. It should be noted that, at the beginning of this plot, the cycles within the data are relatively uniform, but become less uniform as the testing continues, along with the increase of damage. Also, it can be seen that there are flat portions of this data, which indicate that a constant load was held for periods of time during testing.

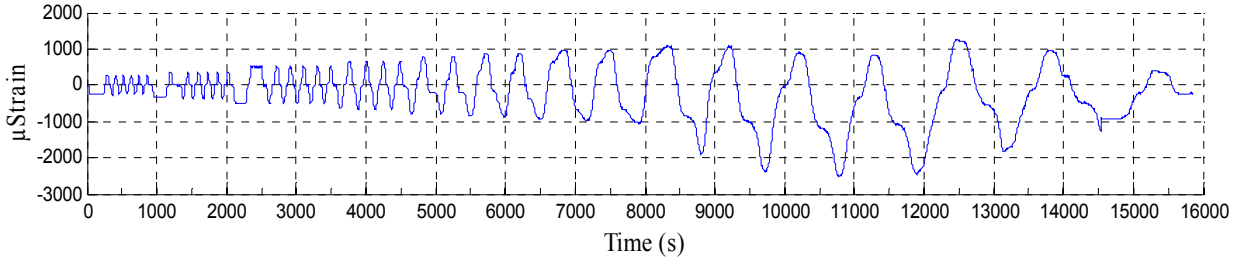

Figure 6. Response at strain gauge 32 versus time

The influence coefficients, EA, and γ values were then calculated for each nodal pair throughout increasing drift sections. Although all of these values are not shown, the EA values for each drift sequence all ranged from 0.95 to 1.00, with the exception of the last drift angle when two coefficient accuracies fell to 0.87 as shown in Table 2. Also, the γ values, not shown, were low for all drifts, at magnitudes of 10^{-4}, confirming the accuracy in estimation of the coefficients.

Table 2. Evalulation accuracy from a 0.07 rad. drift cycle

	32	33	34	35	36
32		0.98	0.98	0.92	0.91
33	0.98		0.98	0.93	0.92
34	0.98	0.98		0.92	0.92
35	0.92	0.93	0.92		0.87
36	0.91	0.92	0.92	0.87	

The initial drifts in which no damage was recorded were taken as the baseline healthy state. Relative deviations of the coefficient values from this baseline were monitored to determine when the method successfully identified the observed damages. Figure 7 shows a visual comparison of the rising changes in the coefficient, $\alpha_{32\text{-}33}$, (i) compared with the noticeable changes in the strain response the two nodes (ii), as severe yielding and cracking of the side plate weld are sustained. The damage associated with each drift sequence is indicated in both plots to give a sense of the graphical changes as they correspond to damage. In Figure 7(i), the influence coefficient value deviates from that of the baseline value. This is consistent with the residual strain that first appears during Damage Class 3 in Figure 7(ii).

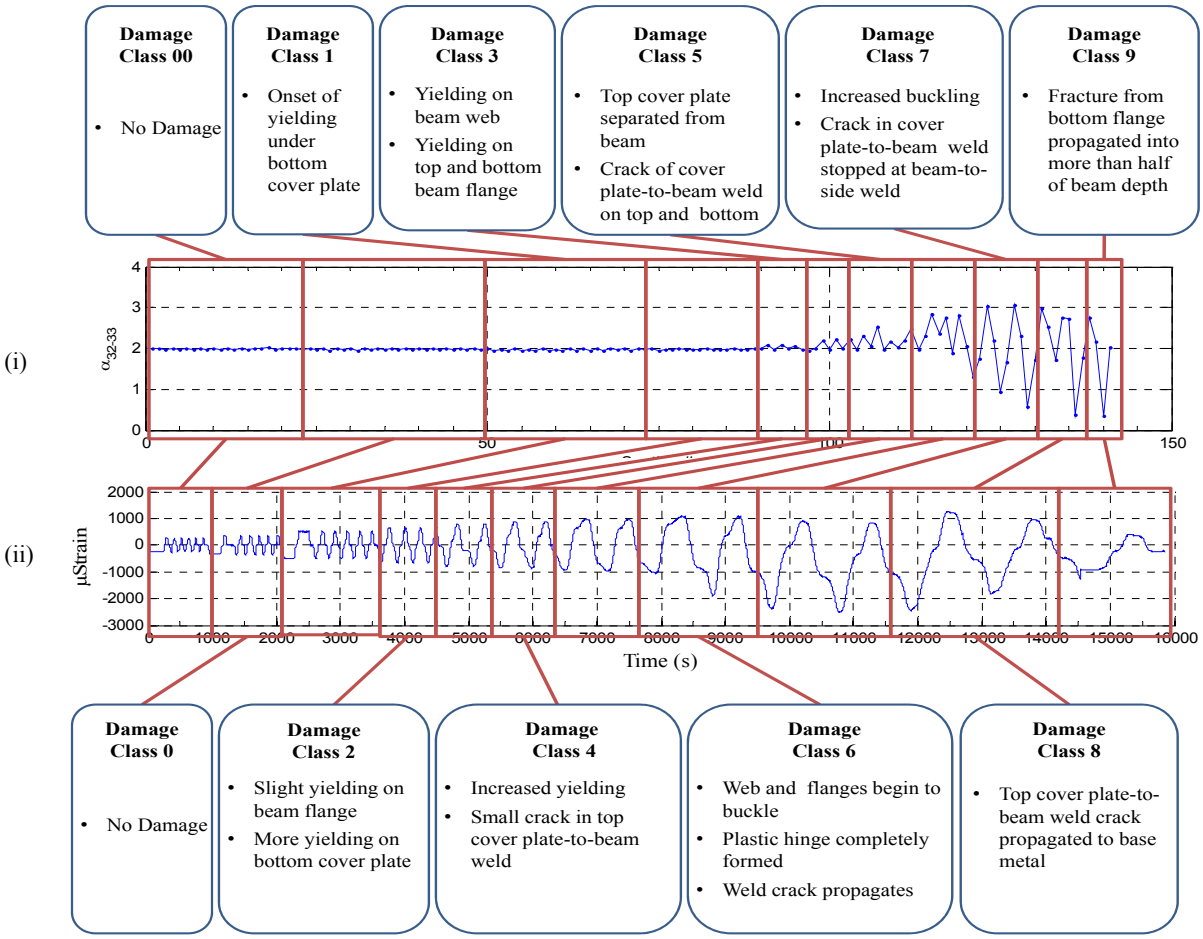

Figure 7. Comparison of damage progression with change in (i) influence coefficients, $\alpha_{32\text{-}33}$, and (ii) strain responses at node 32 over time

For a more quantifiable comaprison, the relative changes were calculated between the coefficients for each damage class and that of the healthy state. The percent change values from each damage class can be seen for select node pairs in Figure 8. The figure also shows the approximate location of damage that occurred during these cycles. According to previous experimental results, the influence coefficients associated with nodes on either side of the damage tend to have a higher percent change compared to those on the same side of the damage [15]. This behavior is supported with the following results as well.

In Figures 8(i) through (iii), all of the percent change values are 3% or less. When comparing these percent change values to the damage which occurred, this is consistent with the mild yielding within the flanges and the bottom cover plate, at the connection. Figures 8(iv) and (v) show higher percent change values around the connection, which reflects the reported increase in damage. The yielding becomes more pronounced, and is located along the connection. However, as Figures 8(vi) through (viii) show, the percent change between sensor 33 and those of both 35 and 36 became lower than expected, showing no significant signs of damage between these nodes. Figure 8(vi), which corresponds to Damage Class 6, is when the plastic hinge completely formed. The resulting out-of-plane bending can be

seen in Figure 9, a view looking up from below the beam. It is possible that node 33 lied within the plastic hinge. This would cause the node to be located on the portion of the beam that would be reverting back to a similar reaction seen near the beginning of the test. The plastic hinge also causes the rest of the beam to contain most of the deformation occurring due to the drift, and, thus, a large portion of the damage is detectable between node pairs 32 with 33 and 34 with 33, as can be seen by the relatively large percent change values. The rest of the values within these figures still indicate that the location of damage is somewhere between sensors 32 and 34 and the connection. When the beam reaches failure due to crack propogation through the bottom flange and halfway up the web, all of the sensors indicate this location of damage at the connection, as is seen with the values in Figure 8(ix). As the crack propagated through the web, it became the dominant damage compared to the plastic hinge, causing sensor 33 to again show percent changes when compared to the column nodes. These parametric changes indicate that the final damage is located somewhere between the beam and the column, or at the connection, as is consistent with the known location of damage.

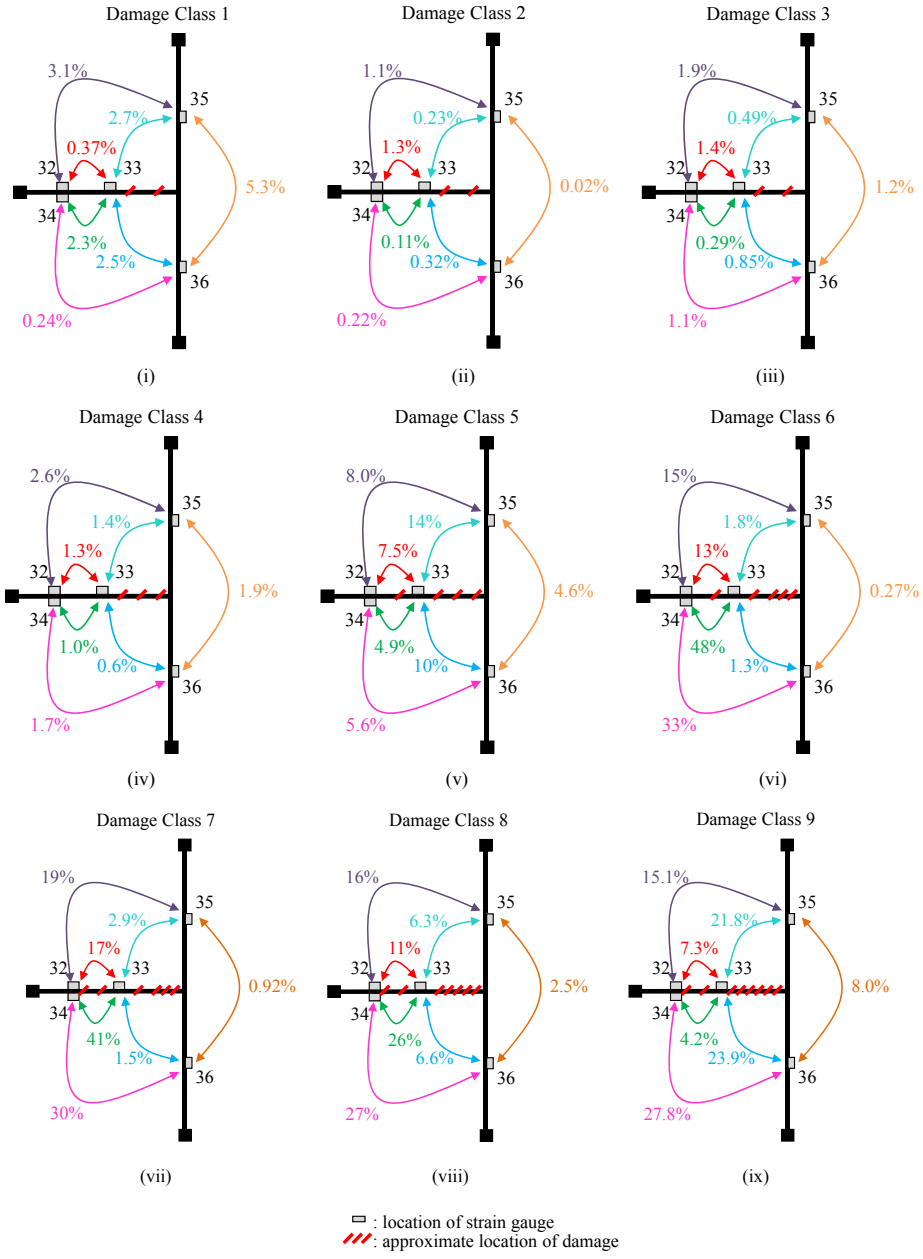

Figure 8. Comparison of relative percent change of influence coefficients as damage progresses with increase in drift angle

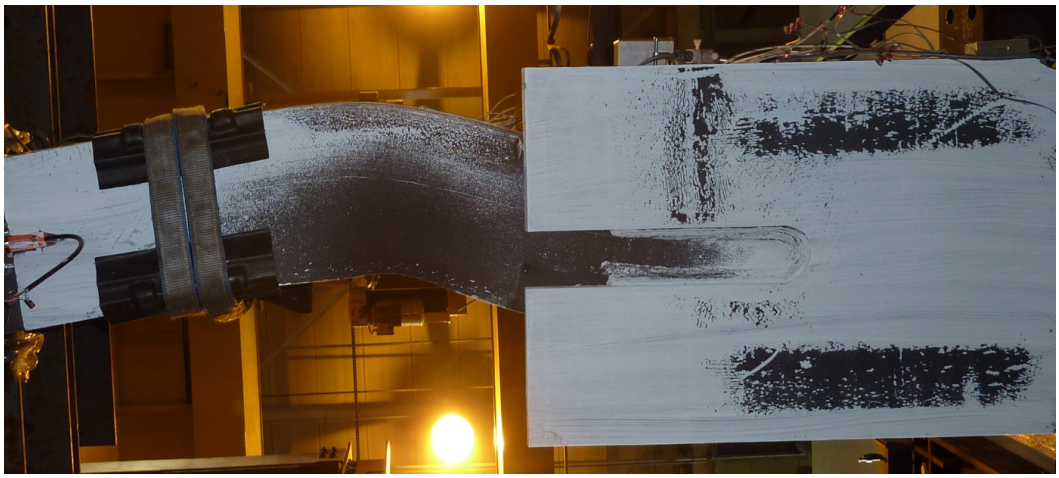

Figure 9. Out-of-plane bending due to plastic hinge formed in the beam, viewed from below

4. CONCLUSIONS

In order to develop SHM methods that are realistic for implementation, it is important to develop methods that are not only applicable to many structure scenarios, but that also utilize affordable and accessible resources. A localize damage detection method based on linear regression analysis that has been previously developed attempts to fulfill this role. This method can be applied to structures that exhibit linear-elastic behavior and that have a baseline condition available, regardless of physical structural properties. While this method has been previously validated for use with both wired and wireless accelerometer sensor networks, the research presented here shows that this method can also be applied using a structure's force response measured with commonly used strain gauges. Furthermore, this paper shows that the method is effective in identifying progressive unknown damage conditions in a large-scale structure. By monitoring the pattern in which the influence coefficients change from the healthy state values, the damage can be localized. It is important to note that in certain damage cases in which the linear-elastic behavior is deviated from, for example the out-of-plane bending due to plastic hinge formation, the damage pattern may not be consistent with the specific location of damage. However, structural damage was localized prior to this state and would ideally be addressed before allowing the structural damage to progress to such a severe state. Ongoing research aims to use statistical confidence bounds to determine the point at which the change in the influence coefficients identifies damage to a significant level.

5. ACKNOWLEDGMENTS

The research described in this paper is partially supported by the National Science Foundation through Grant No. CMMI-0926898 by Sensors and Sensing Systems program, and by a grant from the Commonwealth of Pennsylvania, Department of Community and Economic Development, through the Pennsylvania Infrastructure Technology Alliance (PITA). SidePlate™ is also gratefully acknowledged for permitting the use of additional strain gauges during testing to allow for the application of this algorithm. Finally, special thanks to the ATLSS Center staff for conducting the testing.

6. REFERENCES

[1] Trimm, Marvin. "An overview of nondestructive evaluation methods." Journal of Failure Analysis and Prevention 3(3), 17-31 (2003).

[2] Straser, E. G. and Kiremidjian, A. S., "A Modular, Wireless Damage Monitoring System for Structures," Technical Report 128, John A. Blume Earthquake Engineering Center, Stanford University, Stanford, CA (1998).

[3] Lynch J. P., Loh K. J., "A summary review of wireless sensors and sensor networks for structural health monitoring," The Shock and Vibration Digest ISSN 0583-1024, vol. 38, pp. 91-128 (2006).

[4] Farrar, C. R., Allen, D. W., Ball, S., Masquelier, M. P., and Park. G, "Coupling Sensing Hardware with Data Interrogation Software for Structural Health Monitoring," Proc. 6th Int'l Symp. Dynamic Problems of Mechanics, Ouro Preto, Brazil (2005).

[5] Crossbow Technology, Inc, "MICAz Wireless Measurement System," San Jose, CA (2007).

[6] Intel Corporation Research, Intel Mote2 Overview, Version 3.0, Santa Clara, CA (2005).

[7] Doebling, S. W., Farrar, C. R., and Prime, M. B., "A Summary Review of Vibration-Based Damage Identification Methods," The Shock and Vibration Digest 30, 91-105 (1998).

[8] Alvandi, A., and Cremona, C. "Assessment of vibration-based damage." Journal of Sound and Vibration 292, 179–202 (2006).

[9] Koh, C.G., See, L.M., and Balendra, T. "Damage Detection of Buildings: Numerical and Experimental Studies." J. Struct. Engrg. 121(8), 1155-1160 (Aug 1995).

[10] Morassi, A., and Rovere, N., "Localizing a Notch in a Steel Frame from Frequency Measurements," J. Engrg. Mech. 123(5), 422-432 (1997).

[11] Sohn, H., and Law, K.H. "A Bayesian Probabilistic Approach for Structure Damage Detection." Earthquake Engineering and Structural Dynamics 26, 1259-1281 (1997).

[12] Ratcliffe, C.P. "Damage Detection Using a Modified Laplacian Operator on Mode Shape Data." Journal of Sound and Vibration 204(3), 505-517 (1997).

[13] Bernal, D., M.ASCE. "Load Vectors for Damage Localization." Journal of Engineering Mechanics, 7-14 (Jan 2002).

[14] Yoon, M.K., Heider, D., Gillespie Jr., J.W., Ratcliffe, C.P., and Crane, R.M., "Local damage detection using the two-dimensional gapped smoothing method." Journal of Sound and Vibration 279, 119-139 (2005).

[15] Labuz, E. L., Chang, M., Pakzad, S., "Local Damage Detection in Beam-Column Connections Using a Dense Sensor Network," Proc. of Structures Congress, Orlando, FL, (2010).

[16] Dorvash, S., Pakzad, S., Labuz, E., Chang, M., Li, X., Cheng, L., "Validation of a Wireless Sensor Network using Local Damage Detection algorithm for Beam-Column Connections," Proc. of SPIE 7647, 191-1911 (2010).

[17] Hodgson, I. C, and Ricles, J. M., "Cyclic Testing of Beam-Column Subassemblages Connected with SidePlate™ Steel Moment Frame Connections." (2010).